Polymer Chemistry

ROYAL SOCIETY OF CHEMISTRY

PAPER

View Article Online
View Journal | View Issue

Cite this: *Polym. Chem.*, 2026, **17**, 1529

Ring-opening (co)polymerization of macrolactones catalyzed by a simple organoaluminum complex of $MeAl(BHT)_2$

Rui Han,[a] Zheng Li [a] and Zhibo Li *[a,b]

Received 20th January 2026,
Accepted 12th March 2026

DOI: 10.1039/d6py00054a

rsc.li/polymers

Degradable aliphatic long-chain polyesters (ALCPEs), obtained from the ring-opening polymerization (ROP) of macrolactones (MLs), have emerged as promising degradable polymers, as they combine the mechanical and thermal properties of polyethylene with the degradability of polyesters. Herein, we report a highly efficient $MeAl(BHT)_2$ catalyst for facile ROP of the bio-based macrolactone ω-pentadecalactone (PDL) and ω-dodecalactone (DDL). This system also enables the one-pot random copolymerization of MLs with ε-caprolactone (ε-CL) and δ-valerolactone (δ-VL), allowing for good control of the melting temperature (T_m) of the resulting copolyesters over a range of 48–95 °C by adjusting the monomer feed ratio. More importantly, well-defined block copolymers such as PDDL-*b*-PLLA, PDDL-*b*-PCL, and PDDL-*b*-PVL can be prepared using a sequential monomer addition strategy. The structures and compositions of these polymers were confirmed by nuclear magnetic resonance (NMR) spectroscopy, differential scanning calorimetry (DSC), and gel permeation chromatography (GPC).

Introduction

In response to the global environmental challenge of "white pollution", environmental degradable material systems represented by aliphatic polyesters have emerged and demonstrated significant application potential.[1–7] A very promising solution lies in the development of aliphatic long-chain polyesters (ALCPEs).[8–14] These innovative materials cleverly mimic the structure of polyethylene by introducing sufficiently long methylene units ($-(CH_2)_n-$) into the molecular chain, earning them the name "polyethylene-like materials".[15–17] Their aliphatic long-chain structure endows them with mechanical strength, toughness, and thermal stability comparable to polyethylene, while the inherent ester bonds in the molecular chain ensure their degradability.[11,14,18–20] For example, PPDL exhibited an 18% weight loss after 280 days in compost at 60 °C.[19]

In terms of the synthesis strategy, the ring-opening polymerization (ROP) of macrolactones (MLs) has become an important route for preparing ALCPEs due to its high atom economy, mild reaction conditions, and precise control over the polymer structure. Compared to small-ring lactones (SLs), the ROP of MLs is thermodynamically less favorable. This stems from the lack of significant ring strain in MLs, where the enthalpy change (ΔH_p) of polymerization approaches zero and the reaction is primarily entropy-driven (ΔS). Efficient ROP of MLs such as ω-pentadecalactone (PDL) and ω-dodecalactone (DDL) typically requires elevated temperatures, highly active catalysts, or an extended reaction time to achieve high conversion, posing an ongoing challenge in polymer synthesis.[14,21]

In recent years, the bio-based monomer PDL has received considerable attention. Its homopolymer, PPDL, exhibits polyethylene-like crystallization behavior due to its regular, long and continuous methylene units and thus possesses excellent thermal and mechanical properties.[20,22–24] Structurally similar to PDL, DDL is a 13-membered ML derived from the terpolymerization of 1,3-butadiene. Our recent research has shown that its homopolymer, PDDL, not only has mechanical strength comparable to PPDL, but also exhibits great toughness.[25,26] However, this polyethylene-like character presents synthetic challenges. The high melting temperature (T_m ≈ 95 °C for PPDL and 85 °C for PDDL) necessitates elevated reaction temperatures to maintain monomer diffusion and prevent premature polymer crystallization. At such temperatures, side reactions like transesterification become prominent, often resulting in a reduced number-average molecular weight (M_n) and broadened molecular weight distribution ($Đ$), thereby complicating the synthesis of high-M_n homopolymers and well-defined block copolymers. Although some previous studies have achieved the ROP of PDL at relatively low tempera-

[a]*Shandong Key Laboratory of High Performance Polyolefin Materials and Recycling, College of Polymer Science and Engineering Qingdao University of Science and Technology Qingdao, Shandong 266042, China. E-mail: zbli@qust.edu.cn*
[b]*Key Laboratory of Optic-electric Sensing and Analytical Chemistry for Life Science, MOE, College of Chemistry and Molecular Engineering, Qingdao University of Science and Technology, Qingdao 266042, China*

tures – for instance, Feijen *et al.* employed yttrium isopropoxide as an initiator to realize the rapid ROP of PDL at 60 °C[27] – increasing the monomer/initiator ratio still required an elevated polymerization temperature or a prolonged reaction time to improve conversion. Tsutsumi *et al.* also realized the ROP of PDL at 60 °C using rare-earth tetrahydroborate.[19] However, few catalysts have been reported to achieve efficient ROP of MLs at low temperatures. Therefore, regardless of whether the polymerization temperature is high or low, the design of highly efficient and suitable catalytic systems remains essential for ROP of MLs.

In the early stages of homopolymerization research on PDL and DDL, enzymatic catalysis was the most reported strategy.[28–33] Although enzymes as catalysts offered mild conditions, its inherent drawbacks, such as poor thermal stability and slow polymerization rates, made it unsuitable for synthesizing high-M_n polymers that meet material performance requirements. To overcome the limitations of enzymatic catalysis, researchers have focused on developing more active catalysts. In recent years, a variety of catalyst systems have been reported and successfully applied to the efficient and controlled ROP of DDL and PDL, including metal catalysts,[10,21–23,34–37] organobase catalysts,[38–43] and Lewis acid–base pairs.[3,44,45] For example, Zhang *et al.* synthesized a series of aluminum-based catalysts that achieved controlled ROP of PDL and the macro(di)lactone ethylene brassylate (EB) and prepared well-defined block copolyesters *via* sequential addition.[21] Liu and collaborators reported an iron(II)-based catalyst for the ROP of PDL and its copolymerization with ε-caprolactone (ε-CL).[36] Hadjichristidis *et al.* used the strong organic base phosphazene (*t*-BuP_4) to catalyze the ROP of PDL and its copolymerization with ε-CL and δ-valerolactone (δ-VL).[43] Our group utilized cyclic trimeric phosphazene base (CTPB) to achieve efficient ROP of PDL and prepared well-defined diblock copolyesters.[41] By controlling the monomer/initiator ratio, we successfully obtained PPDL with a M_n of up to 95.7 kDa and mechanical properties comparable to polyethylene.[20] Later, we prepared high molecular weight PDDL using a binary catalyst of diethylzinc ($ZnEt_2$) and 1,8-diazabicyclo[5.4.0]undec-7-ene (DBU).[25] Despite these advances, the development of new catalytic systems that combine high activity and high controllability for the efficient polymerization and precise sequence control of macrolactones is still desirable.

Recently, our group reported a simple organoaluminum complex, namely MeAl(BHT)$_2$ (BHT = 2,6-di-*tert*-butyl-4-methylphenoxy) (Scheme 1), and applied it to the chemoselectivity and controlled ROP of functional α-methylene-δ-valerolactone (MVL). We demonstrated that MeAl(BHT)$_2$ displayed exceptionally high activity in contrast to the traditional organoaluminum catalyst MeAl[Salen] (where salen is *N*,*N*′-bis(salicylaldimine)-1,2-ethylenediamine, Scheme S1).[46] Moreover, this simple organoaluminum complex can efficiently catalyze the ROP of ε-CL, enabling poly(ε-caprolactone) (PCL) with an ultrahigh M_n of 448.9 kDa.[47] These results inspired us to realize the ROP of PDL and DDL using MeAl(BHT)$_2$ as the catalyst, expand the catalytic system for the ROP of MLs, and thereby promote the process of large-scale synthesis of polyolefin-like materials from MLs. Herein, we employed MeAl(BHT)$_2$ as the catalyst for ROP of PDL or DDL (Scheme 1). Furthermore, random copolyesters with a customized T_m could be easily prepared by one-pot copolymerization of PDL/DDL and SLs. By sequentially adding MLs and L-lactide (L-LA), ε-CL, or δ-VL, well-defined diblock copolymers could be easily prepared.

Results and discussion

ROP of MLs catalyzed by a metal-based catalyst

Under bulk polymerization conditions, we first evaluated the catalytic performance of classical metal catalysts MeAl[Salen], diethylzinc ($ZnEt_2$), tin(II) octoate [Sn(Oct)$_2$], and MeAl(BHT)$_2$ in the ROP of DDL. In general, the catalyst was pre-mixed with benzyl alcohol (BnOH) before adding the DDL monomer, and the reaction was carried out at 130 °C for a prescribed time. It was found that Sn(Oct)$_2$ showed low catalytic activity, with only 17% DDL conversion after 7 hours (Table 1, run 1). In contrast, $ZnEt_2$, MeAl[Salen], and MeAl(BHT)$_2$ exhibited comparable activities, reaching conversions of 88%, 99%, and 89%, respectively (Table 1, runs 2, 3, and 6). Apparently, MeAl(BHT)$_2$ demonstrates very high activity comparable to or slightly lower than conventional metal catalysts for DDL polymerization,

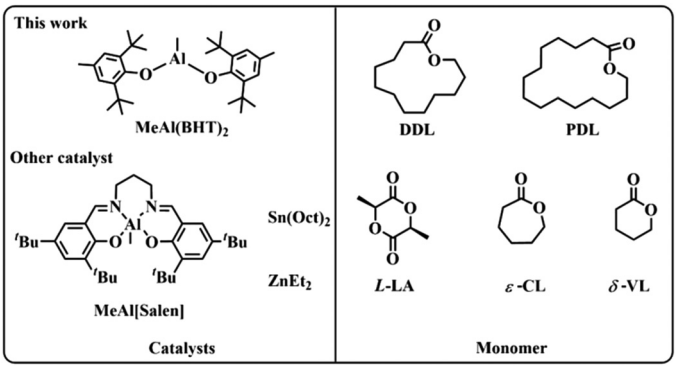

Scheme 1 The structures of the MeAl(BHT)$_2$ in this work and other catalysts and monomers in this study.

Table 1 ROP of DDL and PDL with a metal-based catalyst[a]

Run	$[M]_0/[I]_0/[C]_0$	Catalyst	ML	Temp. (°C)	$[M]_0$ (mol L^{-1})	Time (h)	Conv.[b] (%)	$M_{n,theo}$[c] (kDa)	$M_{n,GPC}$[d] (kDa)	$Đ$[d]
1	100/1/1	$Sn(Oct)_2$	DDL	130	Bulk	7.0	17	3.4	N.A.[e]	N.A.[e]
2	100/1/1	$ZnEt_2$	DDL	130	Bulk	4.0	88	17.5	18.6	2.09
3	100/1/1	MeAl[Salen]	DDL	130	Bulk	4.0	99	19.7	20.6	1.91
4	100/1/1	$MeAl(BHT)_2$	DDL	80	Bulk	9.0	82	16.3	18.7	1.93
5	100/1/1	$MeAl(BHT)_2$	DDL	100	Bulk	6.0	82	16.3	29.2	1.84
6	100/1/1	$MeAl(BHT)_2$	DDL	130	Bulk	4.0	89	17.7	44.4	1.60
7	100/1/1	$MeAl(BHT)_2$	DDL	160	Bulk	2.0	98	19.5	23.3	1.92
8	100/1/1	$MeAl(BHT)_2$	DDL	100	1.0	72.0	33	6.6	4.0	3.56
9	100/1/1	$MeAl(BHT)_2$	DDL	100	2.0	72.0	54	10.8	6.9	3.11
10	50/1/1	$MeAl(BHT)_2$	DDL	130	Bulk	2.0	97	9.7	20.8	1.80
11	200/1/1	$MeAl(BHT)_2$	DDL	130	Bulk	8.0	64	25.5	48.9	1.61
12	300/1/1	$MeAl(BHT)_2$	DDL	130	Bulk	72.0	77	45.8	37.8	1.97
13	100/1/1	$MeAl(BHT)_2$	PDL	100	Bulk	6.0	97	23.4	43.8	1.63
14	100/1/1	$MeAl(BHT)_2$	PDL	130	Bulk	4.0	98	23.6	44.3	1.69
15	100/1/1	$MeAl(BHT)_2$	PDL	160	Bulk	2.0	98	23.6	45.7	1.70
16	50/1/1	$MeAl(BHT)_2$	PDL	130	Bulk	0.5	93	11.3	26.9	1.67
17	200/1/1	$MeAl(BHT)_2$	PDL	130	Bulk	21.0	78	37.6	46.6	1.53

[a] Conditions: $[M]_0/[I]_0/[C]_0$ = monomer/initiator/catalyst. [b] Determined by ^1H NMR. [c] The theoretical M_n was calculated based on: $M_{n,theo} = ([M]_0/[I]_0) \times$ Conv.% × (molecular weight of monomer) + (molecular weight of BnOH). [d] Determined by GPC at 40 °C in chloroform relative to polystyrene standards. [e] The M_n is low, so it is not determined.

while offering the advantages of facile synthesis without requiring intricate ligand design or purification steps. Furthermore, our previous work confirmed that the ROP of lactones catalyzed by $MeAl(BHT)_2$ follows a coordination–insertion mechanism.[46,47]

Subsequently, we focused on the reaction conditions for the ROP of DDL with $MeAl(BHT)_2$ as the catalyst. Fixing the $[M]_0/[I]_0/[C]_0$ = 100/1/1, the effects of temperature on the polymerization were investigated under bulk conditions. At 80 °C, DDL reached 82% conversion after 9 h (Table 1, run 4). Elevating the temperature to 100 °C gave 82% conversion in 6 h (Table 1, run 5). At 130 °C, 89% conversion was achieved in 4 h (Table 1, run 6), while at 160 °C, 98% conversion was obtained within only 2 h (Table 1, run 7). It demonstrated that the polymerization rate increased significantly as the temperature increased from 80 °C to 160 °C. A plot of $\ln[([M]_0 - [M]_e)/([M]_t - [M]_e)]$ *versus* time showed that the apparent rate constant (k_{app}) increased with temperature increase (Fig. S6). Subsequently, we also studied the effects of temperature on the $MeAl(BHT)_2$-catalyzed ROP of PDL (Table 1, runs 13–15). The plot of $\ln[([M]_0 - [M]_e)/([M]_t - [M]_e)]$ *versus* time showed a similar temperature dependence for the ROP of PDL (Fig. S7).

Next, the relationship between conversion and reaction time was investigated for the bulk polymerization at 100 °C. As the polymerization time increased from 0.5 to 2, 3, 4, and 6 h, the DDL conversion increased from 38% to 59%, 70%, 75%, and 82%, respectively (Table S1). The M_n of the resulting PDDL showed a linear increase with monomer conversion (Fig. 1a). The kinetic study of the DDL ROP catalyzed by the $MeAl(BHT)_2$/BnOH system at 100 °C confirmed that the polymerization follows first-order kinetics, with a k_{app} of 0.342 h^{-1} and a half-life ($t_{1/2}$) of about 2 h (Fig. 1b). Under the same conditions, the ROP of PDL also exhibited first-order kinetics, but with a larger rate constant (k_{app} = 0.633 h^{-1}) and a $t_{1/2}$ of only 1.1 h (Fig. S3). Under the same conditions, the polymerization rate of PDL is higher than that of DDL, which may be attributed to the lower activation energy required to reach the transition state during the ROP and chain propa-

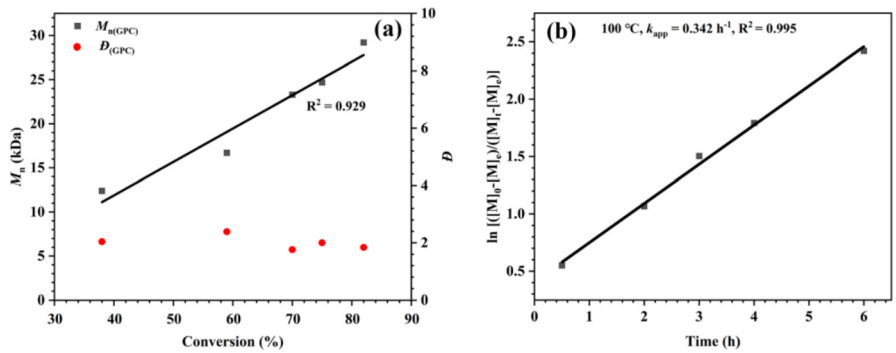

Fig. 1 (a) M_n and $Đ$ of the resultant PDDL *versus* monomer conversion ($[M]_0/[I]_0/[C]_0$ = 100/1/1, $[M]_0$ = bulk, T = 100 °C). (b) Kinetic plots of $\ln[([M]_0 - [M]_e)/([M]_t - [M]_e)]$ *vs.* time ($[M]_0/[I]_0/[C]_0$ = 100/1/1, $[M]_0$ = bulk, T = 100 °C) of DDL.

gation of PDL, resulting in a lower overall energy barrier for the polymerization.

Given the entropy driven ROP of macrolactones, the monomer concentration is another important factor affecting the ROP of MLs. At 100 °C, when the monomer concentration was reduced from bulk to 2 mol L^{-1} and 1 mol L^{-1} in toluene, the polymerization rate decreased significantly, with conversions of only 54% and 33% after 72 h, respectively (Table 1, runs 8 and 9). Owing to the prolonged polymerization time and low monomer conversion, PDDL obtained at reduced monomer concentration exhibited a relatively broader $Đ$.

To control the M_n of PDDL, we fixed the ratio of $[MeAl(BHT)_2]_0/[BnOH]_0$ at 1/1 and varied the $[DDL]_0/[BnOH]_0$ feed ratio at 130 °C. When this ratio was changed from 50/1 to 100/1, 200/1, and 300/1 (Table 1, runs 6, 10–12), the corresponding monomer conversions were 97%, 89%, 64%, and 77%, respectively. The corresponding M_ns of the polymers increased from 20.8 to 44.4 and 48.9 kDa, and then decreased to 37.8 kDa (Fig. 2a). The monomer conversion decreased with increasing $[DDL]_0/[BnOH]_0$ ratio, so the M_n did not increase linearly with the ratio. We believe that the decrease in polymerization efficiency with the increase in the monomer/catalyst ratio is mainly attributed to the purity of the monomer and the insufficient catalytic activity of $MeAl(BHT)_2$ to achieve high conversion. Even when the ratio of $[DDL]_0/[BnOH]_0$ was 300/1, the monomer conversion increased slightly by prolonging the polymerization time. However, more severe transesterification led to a broader $Đ$ (1.97) and thus M_n was not increased. These results indicated that the ROP of DDL catalyzed by $MeAl(BHT)_2$ is not well controlled. Similarly, PPDL with different M_n values was successfully prepared by adjusting the $[PDL]_0/[BnOH]_0$ ratio (Table 1, runs 14, 16, and 17). ^{1}H NMR and MALDI-TOF mass spectrometry confirmed the chain structure of the low-M_n PDDL. In the ^{1}H NMR spectrum, the characteristic signals with equal integration of the α-methylene protons of the hydroxyl end-group (–CH_2OH) at 3.62 ppm and the methylene protons of the benzyloxy group (–O$CH_2C_6H_5$) at 5.11 ppm confirmed the formation of linear PDDL (Fig. S1). The MALDI-TOF MS analysis of low-M_n PDDL showed peaks corresponding to both linear and cyclic polymers adducted with sodium as the cation. The main peaks corresponded to linear PDDL with BnO- end-groups [M_n = 198.31n + 108.14 + 23 (Na^+) g mol^{-1}], while minor peaks indicated the presence of low-M_n cyclic PDDL without chain ends [M_n = 198.31n + 23 (Na^+) g mol^{-1}] (Fig. 2b).

Copolymerization of MLs with L-LA catalyzed by $MeAl(BHT)_2$

We also investigated the copolymerization behaviors of DDL with L-LA in detail. First, at 130 °C, the $MeAl(BHT)_2$/BnOH system showed extremely high activity for the ROP of L-LA. When a pre-mixed $MeAl(BHT)_2$/BnOH solution was added to an L-LA solution ($[L\text{-}LA]_0$ = 4.4 mol L^{-1}), 87% conversion was reached within 20 minutes, and the resulting poly(L-lactic acid) (PLLA) had a narrow $Đ$ value (1.14) (Table 2, run 1). One-pot copolymerization of DDL and L-LA in equal feedstock ratio showed near-complete polymerization of L-LA after 6 h, however with negligible incorporation of DDL (Table 2, run 2). This indicated that DDL and L-LA cannot be copolymerized *via* a one-pot method, consistent with previous studies.[25,26,41] This is because the growing PLLA chain end shows essentially no reactivity toward DDL or PDL. Based on these results, we turned to a sequential monomer addition strategy (Table 2, run 4). According to the GPC curve shown in Fig. 3a, the M_n of the resulting copolymers increased from 17.0 kDa to 22.4 kDa (Table 2, runs 1 and 4).

By changing the $[DDL]_0/[L\text{-}LA]_0/[BnOH]_0$ ratio from 10/100/1 to 50/100/1 and 100/100/1 (Table 2, runs 3–5), the M_n of the corresponding copolymers increased from 16.8 kDa to 22.4 kDa and 33.3 kDa, respectively (Fig. 3a, red, blue, and green curves). These results showed that the M_n and block composition of the copolymers can be easily tuned.

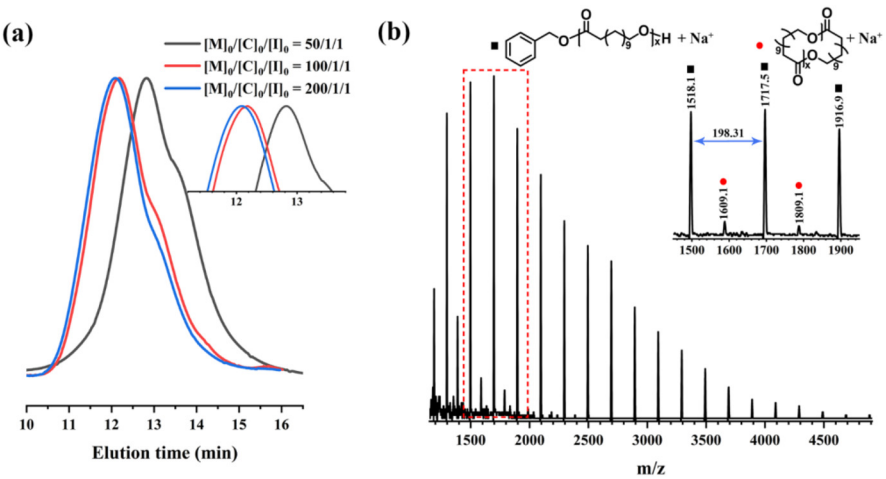

Fig. 2 (a) GPC curves of PDDL samples with different M_n synthesized from different DDL/BnOH feed ratios (in Table 1, runs 6, 10 and 11). (b) MALDI-TOF mass spectrum of PDDL (Table S1, run 1).

Table 2 Copolymerization of DDL or PDL with L-LA catalyzed by $MeAl(BHT)_2$ [a]

Run	$[ML]_0/[L\text{-}LA]_0/[I]_0/[C]_0$	Time (min)	$Conv._{MLs}$ [b] (%)	$Conv._{L\text{-}LA}$ [b] (%)	$M_{n,theo}$ (kDa)	$M_{n,GPC}$ [c] (kDa)	$Đ$ [c]
1	0/100/1/1	20	—	87	12.6	17.0	1.14
2[d]	100/100/1/1 (one-pot)	360	0	95	13.8	19.3	1.52
3[e]	10/100/1/1 (DDL + L-LA)	30 + 60	85	95	15.5	16.8	1.47
4[e]	50/100/1/1 (DDL + L-LA)	120 + 60	90	87	21.5	22.4	1.49
5[e]	100/100/1/1 (DDL + L-LA)	240 + 120	91	76	29.1	33.3	1.73
6[f]	50/100/1/1 (PDL + L-LA)	60 + 90	95	73	22.0	36.1	2.10

[a] Conditions: $[M]_0 = [DDL]_0 + [L\text{-}LA]_0 = 4.4$ mol L^{-1}, $T = 130$ °C. [b] Determined by ^1H NMR. [c] Determined by GPC at 40 °C in chloroform relative to polystyrene standards. [d] One-pot addition of DDL and L-LA. [e] The monomers were added in the order of DDL first, followed by L-LA. [f] The ML was PDL, the monomers were added in the order of PDL first, followed by L-LA, $[M]_0 = [PDL]_0 + [L\text{-}LA]_0 = 3.0$ mol L^{-1}.

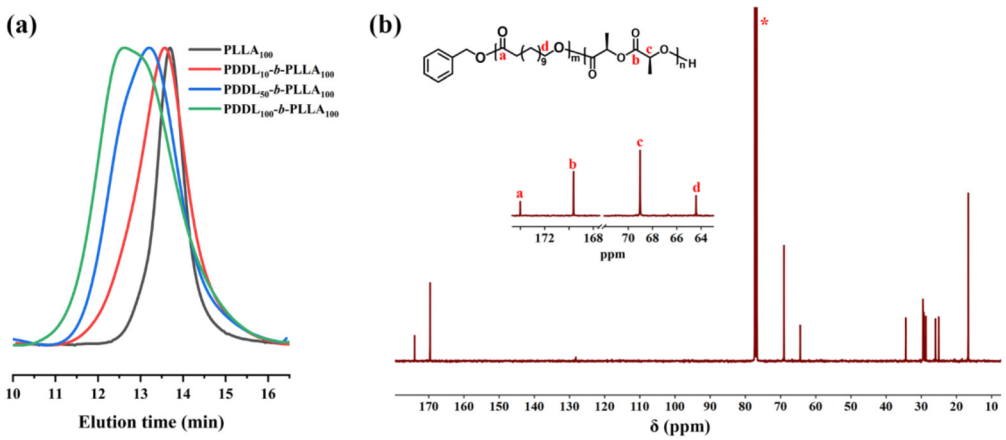

Fig. 3 (a) GPC curves of PLLA (Table 2, run 1) and diblock copolyesters (Table 2, runs 3–5). (b) ^{13}C NMR spectrum of the block copolyester PDDL-*b*-PLLA (Table 2, run 4), solvent: $CDCl_3$.

The obtained copolyesters were characterized by ^1H NMR (Fig. S8). The signals corresponding to the benzyl protons of the $-OCH_2C_6H_5$ group, the methylene protons ($-CH_2-O$) of the PDDL block, and the methine protons ($-CH-O$) of the PLLA block appeared at 5.11, 4.05, and 5.17 ppm, with integrated intensities of approximately 2, 66, and 135, respectively. These results indicated that the copolymer contains about 33 units of DDL and 67 units of L-LA. Both of these values were relatively lower than the theoretical values (DDL: 45 = 50 × 90%, L-LA: 87 = 100 × 87%; Table 2, run 4), which may be due to the formation of a small amount of low-molecular-weight polymers that were removed during precipitation. The ^{13}C NMR spectrum confirmed the successful synthesis of the PDDL-*b*-PLLA diblock copolymer. In the carbonyl region (δ = 174.0 and 169.6 ppm) and the methylene region (δ = 69.0 and 64.4 ppm), only the characteristic peaks corresponding to DDL-DDL and LA–LA sequences were observed, with no signals from cross-sequences (Fig. 3b). DSC analysis showed that when the $[DDL]_0/[L\text{-}LA]_0$ ratio was 10/100 and 50/100, the copolymers exhibited two independent T_ms belonging to the PDDL and PLLA blocks (Fig. 4b, red and blue curves), respectively. However, when the $[DDL]_0/[L\text{-}LA]_0$ ratio was 100/100, only the T_m of the PDDL block at about 83 °C was observed (Fig. 4b, green curve). This was because the crystallization of the PDDL-block effectively inhibited the crystallization of the PLLA-block, a mechanism similar to the observed inhibition of PLLA-block crystallization in PE-*b*-PLLA copolymers, where the covalent linkage and the molten PE-block significantly retard the crystallization kinetics of the PLLA-block.[48,49] The DOSY NMR experiment of the precipitated polymer (Fig. S25; Table 2, run 4) showed two logarithms of diffusion coefficient ($\log D$) that were quite close in the vertical axis. The result suggested the successful synthesis of a PDDL-*b*-PLLA diblock copolyester, but the presence of small amounts of homopolymers cannot be excluded. Similar results were obtained for the sequential copolymerization of PDL with L-LA, successfully preparing well-defined PPDL-*b*-PLLA block copolymers (Table 2, run 6; Table S3; Fig. S10–S13).

Copolymerization of MLs with ε-CL/δ-VL

Then, we investigated the copolymerization behavior of DDL with ε-CL. Typically, a mixed solution of DDL and ε-CL (total monomer concentration: 4.4 mol L^{-1}) was added to the $MeAl(BHT)_2$/BnOH miture solution. Due to severe signal overlap in the ^1H NMR spectrum, only the total conversion of DDL and ε-CL could be determined. After stirring at 130 °C for 1 h, the total monomer conversion reached 84% (Table 3, run 4). Sequence analysis by ^{13}C NMR revealed four signal peaks in the methylene region, corresponding to the DDL–CL, DDL–DDL, CL–CL, and CL–DDL linkages at 64.5, 64.4, 64.1, and

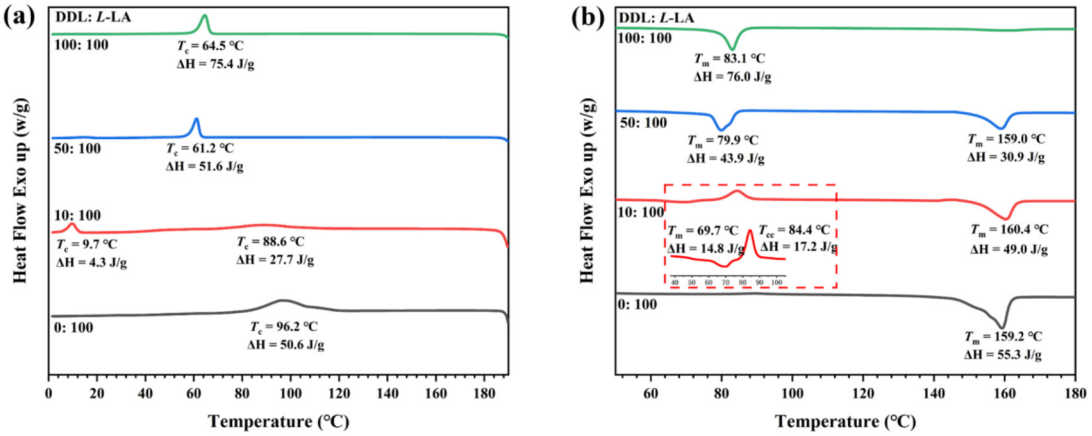

Fig. 4 DSC thermograms of (a) the cooling run with a cooling rate of 10 °C min^{-1} and (b) the second heating run with a heating rate of 10 °C min^{-1} for different [DDL]$_0$/[L-LA]$_0$ ratios. [DDL]$_0$:[L-LA]$_0$ = 100:100 (Table 2, run 5); [DDL]$_0$:[L-LA]$_0$ = 50:100 (Table 2, run 4); [DDL]$_0$:[L-LA]$_0$ = 10:100 (Table 2, run 3); neat PLLA (Table 2, run 1).

Table 3 Copolymerization of DDL or PDL with ε-CL catalyzed by MeAl(BHT)$_2$ [a]

Run	$[ML]_0/[\varepsilon\text{-CL}]_0/[I]_0/[C]_0$	Time (min)	Conv. [b] (%)	$M_{n,theo}$ (kDa)	$M_{n,GPC}$ [c] (kDa)	$Đ$ [c]
1	0/100/1/1	10	99	11.4	32.4	1.53
2[d]	10/100/1/1/1 (one-pot)	20	95	12.8	24.3	1.64
3[d]	50/100/1/1/1 (one-pot)	30	85	18.2	28.5	1.55
4[d]	100/100/1/1/1 (one-pot)	60	84	26.3	57.3	1.46
5[e]	100/100/1/1/1 (DDL + ε-CL)	240 + 60	96	30.1	53.9	2.10
6[f]	100/100/1/1/1 (PDL + ε-CL)	360 + 180	95	33.7	45.0	2.82

[a] Conditions: $[M]_0 = [DDL]_0 + [\varepsilon\text{-CL}]_0$ = 4.4 mol L^{-1}; T = 130 °C. [b] Total conversion of ML and ε-CL determined by ^{1}H NMR. [c] Determined by GPC at 40 °C in chloroform relative to polystyrene standards. [d] One-pot addition of DDL and ε-CL. [e] The monomers were added in the order of DDL first, followed by ε-CL. [f] The ML was PDL, the monomers were added in the order of PDL first, followed by ε-CL, $[M]_0 = [PDL]_0 + [\varepsilon\text{-CL}]_0$ = 2.0 mol L^{-1}; T = 100 °C.

64.0 ppm, respectively (Fig. 5a). The integrations of these four signals were 0.20, 0.21, 0.38, and 0.21, which highly matched the theoretical distribution for a random copolymer (Fig. S14).

Furthermore, DSC analysis showed that the obtained copolymer gave a single T_m at 58.1 °C (Fig. 6, blue curve), which is intermediate between that of PDDL ($T_m \approx 85$ °C)[26,43] and PCL (T_m = 60 °C),[34] indicating the random distribution of DDL and ε-CL units in the copolyester chain. By changing the monomer feed ratio, copolyesters with tunable M_n and T_ms could be easily obtained (Table 3, runs 2–4; Fig. 6). Random copolymers of DDL and CL exhibit high crystallinity over the entire composition range, which is attributed to the cocrystallization of the

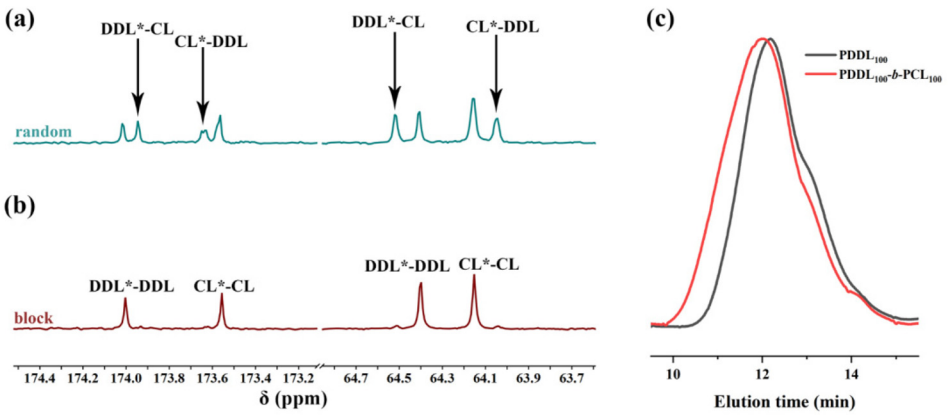

Fig. 5 ^{13}C NMR spectra of (a) the random copolyester PDDL-*ran*-PCL (Table 3, run 4) and (b) the block copolyester PDDL-*b*-PCL (Table 3, run 5), solvent: $CDCl_3$. (c) GPC curves of PDDL (Table 1, run 6) and copolyesters (Table 3, run 5).

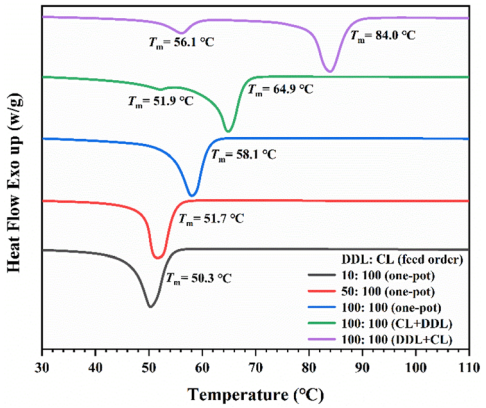

Fig. 6 DSC thermograms of the second heating run for copolyester of DDL/ε-CL: PDDL-*ran*-PCL (black spectrum, Table 3, run 2); PDDL-*ran*-PCL (red spectrum, Table 3, run 3); PDDL-*ran*-PCL (blue spectrum, Table 3, run 4); PDDL-*ran*-PCL (green spectrum, Table S4, run 3); PDDL-*b*-PCL (purple spectrum, Table 3, run 5).

CL and DDL comonomer units.[50,51] Interestingly, even when a sequential monomer addition method was employed, *i.e.*, ROP of ε-CL first before adding DDL, the obtained products were random or multi-block like copolymers, indicating that significant transesterification reactions occurred during the copolymerization (Table S4, runs 1–3; Fig. 6, green curve). The copolymerization of PDL with ε-CL also exhibited the same behavior (Table S4, runs 7–12; Fig. S16a and S17). The distinct behaviors of L-LA and ε-CL as the first block in initiating macrolactone polymerization arise from the fundamental difference in their active centers: L-LA generates a secondary alkoxide anion, while ε-CL forms a primary alkoxide anion. Thus, the PCL chain end remains reactive enough to initiate the polymerization of macrolactones.

In sharp contrast, if we performed ROP of DDL first before adding ε-CL, well-defined block copolymers were successfully obtained. For example, the ROP of DDL was conducted at 130 °C for 4 h, and then ε-CL was added to the reaction mixture. The ROP of ε-CL was completed within 1 h, with a monomer conversion of 96% (Table 3, run 5). Compared to the PDDL-*ran*-PCL random copolyester, ^{13}C NMR spectrum analysis showed only two characteristic peaks in the carbonyl region at 174.0 and 173.5 ppm, corresponding to the DDL–DDL and CL–CL linkages, with no cross-sequence signals (Fig. 5b).

Through DSC analysis, the thermogram showed two distinct T_m values at 56.1 °C and 84.0 °C, corresponding to the PCL-block and PDDL-block domains, respectively (Fig. 6, purple curve). Furthermore, the GPC curve of the corresponding copolyester shifted toward higher molecular weight (Fig. 5c). These pieces of evidence collectively demonstrate the successful synthesis of the PDDL-*b*-PCL diblock copolymer. The DOSY NMR experiment of the precipitated polymer (Fig. S26; Table 3, run 5) showed only one log D in the vertical axis. These results suggested the successful synthesis of a PDDL-*b*-PCL diblock copolyester, but the presence of small amounts of homopolymers cannot be excluded. Similarly, a PPDL-*b*-PCL block copolyester was also successfully synthesized *via* this strategy (Table 3, run 6; Fig. S15, S16b, and S17).

Under identical sequential polymerization conditions (DDL first, then ε-CL), MeAl[Salen] and $ZnEt_2$ yielded copolyesters with distinct sequence structures. Both achieved high monomer conversions (>97%, Table S4, runs 15 and 16). ^{13}C NMR analysis showed four methylene signals for each copolymer (Fig. S19). For the MeAl[Salen] product, the peak integrals (0.19, 0.32, 0.33, 0.17) matched a random sequence, and DSC displayed a single T_m at 68.6 °C (Fig. S20 and S18, black curve). In contrast, the $ZnEt_2$ product exhibited integrals (0.06, 0.45, 0.43, 0.06) indicating partial blocking, and its DSC showed two T_m values (55.2 °C and 79.9 °C), corresponding to PCL and PDDL segments (Fig. S21 and S18, red curve). Thus, MeAl[Salen] produced a fully random copolymer, while $ZnEt_2$ gave a material with blocky features yet accompanied by significant transesterification, as evidenced by the lowered T_m of the PDDL block.

Finally, we extended our study to the copolymerization of DDL and PDL with δ-VL. The experimental results were highly similar to those of the ε-CL system: the one-pot method or the sequential addition of polymerizing δ-VL first both yielded random copolymers (Table 4, runs 2–4; Table S5, runs 1–3, 7–12; Fig. 7a, 8 and Fig. S24), whereas the sequential addition strategy of polymerizing DDL or PDL first successfully produced well-defined PDDL-*b*-PVL and PPDL-*b*-PVL diblock copolymers (Table 4, runs 5, 6). Their block structure was con-

Table 4 Copolymerization of DDL or PDL with δ-VL catalyzed by MeAl(BHT)$_2$[a]

Run	$[ML]_0/[\delta\text{-VL}]_0/[I]_0/[C]_0$	Time (min)	Conv.[b] (%)	$M_{n,theo}$ (kDa)	$M_{n,GPC}$[c] (kDa)	$Đ$[c]
1	0/100/1/1	10	96	9.7	21.7	1.30
2[d]	10/100/1/1/1 (one-pot)	20	94	11.4	19.7	1.45
3[d]	50/100/1/1/1 (one-pot)	30	90	18.0	21.0	1.68
4[d]	100/100/1/1/1 (one-pot)	60	86	25.7	39.1	1.49
5[e]	100/100/1/1/1 (DDL + δ-VL)	240 + 60	85	25.4	35.3	1.71
6[f]	100/100/1/1/1 (PDL + δ-VL)	360 + 180	81	27.6	49.8	2.05

[a] Conditions: $[M]_0 = [DDL]_0 + [\delta\text{-VL}]_0 = 4.4$ mol L^{-1}; $T = 130$ °C. [b] Total conversion of ML and δ-VL determined by ^{1}H NMR. [c] Determined by GPC at 40 °C in chloroform relative to polystyrene standards. [d] One-pot addition of DDL and δ-VL. [e] The monomers were added in the order of DDL first, followed by δ-VL. [f] The ML was PDL, the monomers were added in the order of PDL first, followed by δ-VL, $[M]_0 = [PDL]_0 + [\delta\text{-VL}]_0 = 2.0$ mol L^{-1}; $T = 100$ °C.

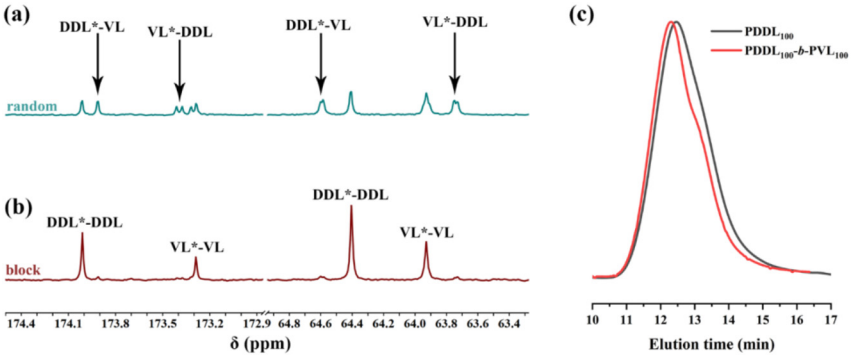

Fig. 7 ^{13}C NMR spectra of (a) PDDL-*ran*-PVL (Table S5, run 3) and (b) PDDL-*b*-PVL (Table 4, run 5), solvent: $CDCl_3$; (c) GPC curves of the PDDL homopolymer (T = 130 °C, monomer conversion was 80%, M_n = 30.1 kDa, $Đ$ = 1.74) and copolyesters (Table 4, run 5).

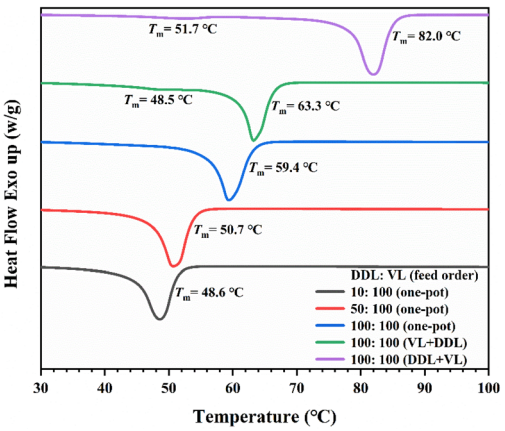

Fig. 8 DSC thermograms of the second heating run for copolyester of DDL/δ-VL: PDDL-*ran*-PVL (black spectrum, Table 4, run 2); PDDL-*ran*-PVL (red spectrum, Table 4, run 3); PDDL-*ran*-PVL (blue spectrum, Table 4, run 4); PDDL-*ran*-PVL (green spectrum, Table S5, run 3); PDDL-*b*-PVL (purple spectrum, Table 4, run 5).

firmed by ^{13}C NMR (Fig. 7b), DSC (Fig. 8), and the shift toward higher M_n of the GPC curves (Fig. 7c). The DOSY NMR experiment of the precipitated polymer (Fig. S27; Table 4, run 5) showed two log D values that were quite close in the vertical axis. These results suggested the successful synthesis of a PDDL-*b*-PVL diblock copolyester, but the presence of small amounts of homopolymers cannot be excluded.

Conclusions

In conclusion, this study demonstrated that $MeAl(BHT)_2$ can be effectively used for the ROP of macrolactones PDL and DDL. The ROP results showed that $MeAl(BHT)_2$ showed high activity for both PDL and DDL. Kinetic studies revealed that the ROP of both PDL and DDL follows first-order kinetics. Subsequently, the random copolymerization of MLs with ε-CL and δ-VL was achieved *via* a one-pot method, allowing the T_m of the resulting copolymers to be tuned within the range of 48–95 °C. More importantly, by employing sequential monomer addition, a series of well-defined diblock copolymers, including PDDL-*b*-PLLA, PDDL-*b*-PCL, and PDDL-*b*-PVL, were successfully synthesized. The block structures were confirmed by NMR spectroscopy, DSC, and GPC. This research not only provides an efficient catalytic system for the synthesis of degradable polyester materials with tunable thermal properties, but also offers new insights for the future design of novel catalysts for the ROP of macrolactones.

Conflicts of interest

There are no conflicts to declare.

Data availability

The data that support the findings of this study are available from the corresponding author upon reasonable request.

Supplementary information (SI): experimental raw data (*e.g.*, NMR spectra, GPC traces, MALDI-TOF-MS results), polymerization reaction conditions and yield records, as well as characterization data of catalysts and polymers; supplementary figures that further detail the experimental procedure data and results. See DOI: https://doi.org/10.1039/d6py00054a.

Acknowledgements

The authors appreciate the National Natural Science Foundation of China (No. U24A20558 and 22401170).

References

1 M. Häußler, M. Eck, D. Rothauer and S. Mecking, *Nature*, 2021, **590**, 423–427.
2 Y. Zhao, E. M. Rettner, K. L. Harry, Z. Hu, J. Miscall, N. A. Rorrer and G. M. Miyake, *Science*, 2023, **382**, 310–314.
3 B. Wang, L. Pan, Z. Ma and Y. Li, *Macromolecules*, 2018, **51**, 836–854.

4 M. Vert, *Biomacromolecules*, 2005, **6**, 538–546.
5 T. Şucu and M. P. Shaver, *Polym. Chem.*, 2020, **11**, 6397–6412.
6 N. A. Mahadas, A. Suhail, M. T. Sobczak, X. Li, K. Chen, K. Song, G. Dong, O. Kuksenok and C. Tang, *Macromolecules*, 2025, **58**, 4070–4081.
7 K. Liu, H. Zhao, N. Ding, C. Chen, X. Jiang, S. Yu, J. Wang, F. Liu and J. Zhu, *Polym. Degrad. Stab.*, 2026, **244**, 111806.
8 P. Ortmann and S. Mecking, *Macromolecules*, 2013, **46**, 7213–7218.
9 M. P. F. Pepels, M. R. Hansen, H. Goossens and R. Duchateau, *Macromolecules*, 2013, **46**, 7668–7677.
10 I. van der Meulen, E. Gubbels, S. Huijser, R. Sablong, C. E. Koning, A. Heise and R. Duchateau, *Macromolecules*, 2011, **44**, 4301–4305.
11 M. P. F. Pepels, L. E. Govaert and R. Duchateau, *Macromolecules*, 2015, **48**, 5845–5854.
12 F. Stempfle, P. Ortmann and S. Mecking, *Chem. Rev.*, 2016, **116**, 4597–4641.
13 T. F. Nelson, D. Rothauer, M. Sander and S. Mecking, *Angew. Chem., Int. Ed.*, 2023, **62**, e202310729.
14 C. Nakornkhet, S. Kamavichanurat, W. Joopor and P. Hormnirun, *Polym. Chem.*, 2024, **15**, 1660–1679.
15 M. Eck, S. T. Schwab, T. F. Nelson, K. Wurst, S. Iberl, D. Schleheck, C. Link, G. Battagliarin and S. Mecking, *Angew. Chem., Int. Ed.*, 2022, **62**, e202213438.
16 H. Janani, S. F. Marxsen, M. Eck, S. Mecking, K. Tashiro and R. G. Alamo, *ACS Macro Lett.*, 2024, **13**, 201–206.
17 S. Xu, Y. Zheng and P. Pan, *ACS Macro Lett.*, 2025, **14**, 1448–1458.
18 H.-Y. Ji, B. Wang, L. Pan and Y.-S. Li, *Green Chem.*, 2018, **20**, 641–648.
19 Y. Nakayama, N. Watanabe, K. Kusaba, K. Sasaki, Z. Cai, T. Shiono and C. Tsutsumi, *J. Appl. Polym. Sci.*, 2011, **121**, 2098–2103.
20 B.-Z. Huang, R. Han, Z. Li and Z.-B. Li, *Acta Polym. Sin.*, 2024, **55**, 976–985.
21 W.-C. Zhao, J. Yuan, J.-H. He and Y.-T. Zhang, *Chin. J. Polym. Sci.*, 2023, **41**, 1706–1713.
22 J. A. Wilson, S. A. Hopkins, P. M. Wright and A. P. Dove, *Biomacromolecules*, 2015, **16**, 3191–3200.
23 D. Myers, T. Witt, A. Cyriac, M. Bown, S. Mecking and C. K. Williams, *Polym. Chem.*, 2017, **8**, 5780–5785.
24 P. Skoglund and A. Fransson, *Polymer*, 1998, **39**, 1899–1906.
25 R. Han, Z. Li and Z. Li, *Eur. Polym. J.*, 2025, **240**, 114339.
26 R. Han, X. Miao, D. Zhao, Z. Li and Z. Li, *Polym. Chem.*, 2025, **17**, 1939–1948.
27 Z. Zhong, P. J. Dijkstra and J. Feijen, *Macromol. Chem. Phys.*, 2000, **201**, 1329–1333.
28 P. Panlawan, P. Luangthongkam, L. O. Wiemann, V. Sieber, E. Marie, A. Durand and P. Inprakhon, *J. Mol. Catal. B: Enzym.*, 2013, **88**, 69–76.
29 C. Li, S. Pan, W. Xu, Y. Lu, P. Wang, F. Zhang and R. A. Gross, *Green Chem.*, 2020, **22**, 662–668.
30 M. Hunsen, A. Abul, W. Xie and R. Gross, *Biomacromolecules*, 2008, **9**, 518–522.
31 M. de Geus, I. van der Meulen, B. Goderis, K. van Hecke, M. Dorschu, H. van der Werff, C. E. Koning and A. Heise, *Polym. Chem.*, 2010, **1**, 525–533.
32 I. V. D. Meulen, M. D. Geus, H. Antheunis, R. Deumens, E. A. J. Joosten, C. E. Koning and A. Heise, *Biomacromolecules*, 2008, **9**, 3404–3410.
33 L. V. D. Mee, F. Helmich, R. D. Bruijn, J. A. J. M. Vekemans, A. R. A. Palmans and E. W. Meijer, *Macromolecules*, 2006, **39**, 5021–5027.
34 M. Bouyahyi and R. Duchateau, *Macromolecules*, 2014, **47**, 517–524.
35 T. Fuoco, A. Meduri, M. Lamberti, V. Venditto, C. Pellecchia and D. Pappalardo, *Polym. Chem.*, 2015, **6**, 1727–1740.
36 L.-J. Liu, W.-P. Zhao, L.-S. Ma, C.-Y. Zhang, F. Wang, X.-Q. Zhang and H. Liu, *Chin. J. Polym. Sci.*, 2025, **43**, 640–654.
37 J. A. Wilson, S. A. Hopkins, P. M. Wright and A. P. Dove, *Polym. Chem.*, 2014, **5**, 2691–2694.
38 M. Bouyahyi, M. P. F. Pepels, A. Heise and R. Duchateau, *Macromolecules*, 2012, **45**, 3356–3366.
39 V. Ladelta, P. Bilalis, Y. Gnanou and N. Hadjichristidis, *Polym. Chem.*, 2017, **8**, 511–515.
40 S. Naumann, A. W. Thomas and A. P. Dove, *ACS Macro Lett.*, 2016, **5**, 134–138.
41 N. Zhao, C. Ren, Y. Shen, S. Liu and Z. Li, *Macromolecules*, 2019, **52**, 1083–1091.
42 R. Todd, S. Tempelaar, G. Lo Re, S. Spinella, S. A. McCallum, R. A. Gross, J.-M. Raquez and P. Dubois, *ACS Macro Lett.*, 2015, **4**, 408–411.
43 V. Ladelta, J. D. Kim, P. Bilalis, Y. Gnanou and N. Hadjichristidis, *Macromolecules*, 2018, **51**, 2428–2436.
44 S. Naumann, P. B. V. Scholten, J. A. Wilson and A. P. Dove, *J. Am. Chem. Soc.*, 2015, **137**, 14439–14445.
45 P. Walther and S. Naumann, *Macromolecules*, 2017, **50**, 8406–8416.
46 Q. Yan, J. Ma, W. Pei, Y. Zhang, R. Zhong, S. Liu, Y. Shen and Z. Li, *Angew. Chem., Int. Ed.*, 2024, **64**, e202418488.
47 Q. Yan, J. Ma, W. Li, S. Liu, Y. Shen and Z. Li, *Macromolecules*, 2025, **58**, 12981–12990.
48 A. J. Müller, R. V. Castillo and M. Hillmyer, *Macromol. Symp.*, 2006, **242**, 174–181.
49 A. J. Müller, A. T. Lorenzo, R. V. Castillo, M. L. Arnal, A. Boschetti-de-Fierro and V. Abetz, *Macromol. Symp.*, 2007, **245–246**, 154–160.
50 Q. Guo, Y. Zhang, H. Ruan, H. Sun, T. Wang, Q. Wang and C. Wang, *Macromol. Rapid Commun.*, 2024, **45**, 2300534.
51 G. Ceccorulli, M. Scandola, A. Kumar, B. Kalra and R. A. Gross, *Biomacromolecules*, 2005, **6**, 902–907.